Geomechanics and Engineering, *Vol. 24, No. 5 (2021) 443-456*
DOI: https://doi.org/10.12989/gae.2021.24.5.443

Three dimensional seismic deformation-shear strain-swelling performance of America-California Oroville Earth-Fill Dam

Memduh Karalar* and Murat Çavuşli[a]

Department of Civil engineering, Zonguldak Bulent Ecevit University Zonguldak, 67100, Turkey

(Received March 23, 2020, Revised February 18, 2021, Accepted February 28, 2021)

Abstract. Structural design of the vertical displacements and shear strains in the earth fill (EF) dams has great importance in the structural engineering problems. Moreover, far fault earthquakes have significant seismic effects on seismic damage performance of EF dams like the near fault earthquakes. For this reason, three dimensional (3D) earthquake damage performance of Oroville dam is assessed considering different far-fault ground motions in this study. Oroville Dam was built in United States of America-California and its height is 234.7 m (770 ft.). 3D model of Oroville dam is modelled using FLAC3D software based on finite difference approach. In order to represent interaction condition between discrete surfaces, special interface elements are used between dam body and foundation. Non-reflecting seismic boundary conditions (free field and quiet) are defined to the main surfaces of the dam for the nonlinear seismic analyses. 6 different far-fault ground motions are taken into account for the full reservoir condition of Oroville dam. According to nonlinear seismic analysis results, the effects of far-fault ground motions on the nonlinear seismic settlement and shear strain behaviour of Oroville EF dam are determined and evaluated in detail. It is clearly seen that far-fault earthquakes have very significant seismic effects on the settlement-shear strain behaviour of EF dams and these earthquakes create vital important seismic damages on the swelling behaviour of dam body surface. Moreover, it is proposed that far-fault ground motions should not be ignored while modelling EF dams.

Keywords: earth-fill dam; far-fault earthquake; free-field boundary condition; interaction condition; shear strain failure

1. Introduction

Nowadays, many types of conventional dams are built in the world such as earth-fill (EF) dam, concrete-faced rockfill dam, and asphalt faced rockfill dam and earth-fill (EF) dams are one of the most significant water constructions for all living creatures. In recent years, these important structures have great interests due to the increase in the rise of environmental awareness and renewable energy. Besides, according to the world's leading engineering and economical researches, this dam type is one of the best choices for the ultimate design. EF dams constructed on the fault zones (far-fault and near-fault) may undergo strong ground motions. For this reason, the seismic performance of this dam type should be investigated considering both far-fault and near fault effects. It is observed that there are many studies about the seismic behavior of dams in the literature. Dynamic analysis of dam-reservoir-foundation system is usually carried out by employing a simplified and approximate one-dimensional model to account for fluid-foundation interaction. The approximation introduced on this basis was examined thoroughly in a study by comparing the method with the rigorous approach. It was concluded that the errors due to approximate method could be very significant both for horizontal and vertical ground motions (Lotfi 2005). Then, same researcher was proposed an efficient procedure for dynamic analysis of concrete a special dam. The accuracy of this technique was examined thoroughly and it was concluded that efficient procedure is incredibly accurate under all practical conditions (Lotfi 2006). Moreover, it was investigated the effect of transient stochastic analysis on nonlinear response of earth and rockfill dams to spatially varying ground motion. Stationary as well as transient stochastic response analyses were performed for the both dam types. It was observed that stationarity is a reasonable assumption for earth and rock-fill dams to typical durations of strong shaking (Haciefendioglu 2006). In addition, it was investigated the ice cover effects on the near fault earthquake behaviour of gravity dams. In the seismic analyses, earthquake loads were applied to the dam model with and without ice cover. According to analysis results, the effects of variations of the thickness, length and elasticity modulus of the ice-cover on the nonlinear displacement and stress behaviour of gravity dams are clearly seen (Haciefendioglu *et al.* 2010). Then, it was examined the seismic principal stress values in the gravity dams. A new equation was proposed taking into account the time domain approach and that equation supports for finding seismic principal stresses in the dam body during near fault earthquake (Akpınar *et al.* 2014). Terzi and Selcuk examined nonlinear dynamic behavior of an earth-fill dam. Numerical analysis showed that this dam is likely to experience moderate deformations during the design earthquake but will remain stable after the earthquake is

*Corresponding author, Assistant Professor
E-mail: memduhkaralar@gmail.com
[a]Ph.D. Student
E-mail: murat.cavusli@beun.edu.tr

ISSN: 2005-307X (Print), 2092-6219 (Online)

applied (Terzi and Selcuk 2015). Then, it was examined nonlinear seismic response of rockfill dams considering different ground motions. The mean of maximum and variance response values obtained from a spatially varying ground motion case are compared with those of specialized ground motion models. It was observed that the variation in local soil conditions has important effects on the nonlinear response of rockfill dams in that study (Haciefendioglu and Soyluk 2016). Besides, it was performed near fault earthquake assessment for rockfill dams. According to earthquake analyses, maximum tensions and minimum tensions occurred in the heel and toe of the dam, respectively (Arefian *et al.* 2016). Cavusli examined static behaviour of Atatürk clay core rockfill dam and it was obtained very important information about static behaviour of clay core rockfill dams (Cavusli 2016). It was carried out a near fault earthquake performance assessment for rockfill dams considering strong ground motions. According to numerical analysis results, strong shaking (approximately 0.7–1.0g) has not significant seismic effects on the safety and future of these dams. Moreover, it was clearly demonstrated that a counterbalancing has very important seismic effects on the earthquake behaviour of the dams (Park and Kim 2017). In addition, it was examined earthquake damage performance of a high rockfill dam considering near-fault pulse-like earthquakes. Nonlinear numerical analysis results showed that although the near-fault pulse-like ground motion significantly affects the acceleration of dam during the earthquake, it has also significant effects on the nonlinear displacement behaviour of rockfill dam (Zou *et al.* 2017). It was investigated near fault earthquake damages of gravity dams taking into account near-field earthquakes. The tallest gravity dam in the world was modelled using the finite element method for the full reservoir condition of the dam. Earthquake performance of the dam was assessed taking into account earthquake fragility curves. As a result of that study, it was clearly seen that the pulse-like and the non-pulse-like earthquakes have very different and significant nonlinear seismic effects on the nonlinear earthquake performance of the gravity dams (Yazdani and Alembagheri 2017). Then, it was assessed near fault earthquake analyses of rockfill dam slopes using probability density evolution method. In that study, a new and significant method was proposed to examine the earthquake reliability analyses of rockfill dams. According to the nonlinear numerical results, it was clearly seen that this proposed method is a very significant approach on the earthquake reliability evaluation of the rockfill dams (Pang *et al.* 2018). Moreover, an approach was proposed for the evaluation of seismic safety behaviour of tailings dams. In that study, it was clearly showed that for low-frequency input ground motions, the seismic safety factor is approximately 26% lower than high-frequency ground motions (Nimbalkar *et al.* 2018). Moreover, it was examined the effects of near-fault ground motion durations on the earthquake behaviour of rockfill dams. Total 40 earthquakes were applied to the dam to assess the nonlinear effects of earthquake duration on the nonlinear earthquake behaviour of rockfill dams. According to numerical results, it was clearly seen that when earthquake duration increase, the settlements and plastic shear strains proportionally rise (Xu *et al.* 2018). Moreover, it was performed near fault earthquake damage analyses of rockfill dams using generalized probability density evolution method. In that study, it was demonstrated that the earthquake characteristic properties create significant differences in the earthquake analyses of dams (Pang *et al.* 2018). Then, an earthquake determination method was proposed to assess the near fault earthquake behaviour of rockfill dams. In the numerical results, it was clearly seen that numerical seismic method has significant seismic effects on the predicting of earthquake damage (Pang *et al.* 2018). A numerical seismic method was examined for evaluation of near fault earthquake behaviour of rockfill dams. It was obviously indicated in that study that water compressibility has significant seismic effects on the principal stress behaviour of these dams (Xu *et al.* 2018). It was proposed an effective approach for deformation behaviour of rockfill dams. The numerical results showed that the pulse-like ground motions have important seismic effects on the displacement behaviour of the rockfill dams. Moreover, it was clearly indicated that if the pulse-like ground motions are ignored during seismic analyses, the inaccurate results may be obtained (Zou *et al.* 2019). Kartal *et al.* assessed settlement behaviour of clay core rockfill dams considering geodetic measurements. It was observed that geodetic settlement data and settlement values obtained from numerical analysis are very close to each other (Kartal *et al.* 2019). There are many studies related with examination of the nonlinear behaviour of rockfill dams in the literature (Noorzad and Omidvar 2010, Seiphoori *et al.* 2011, Dakoulas 2012, Zou *et al.* 2013, Yang and Chi 2014, Albano *et al.* 2015, Lin *et al.* 2015, Chen *et al.* 2016, Han *et al.* 2016, Cen *et al.* 2016, Wang *et al.* 2018, Karalar and Cavusli 2018, Karalar and Cavusli 2018, Hu and Huang 2019, Karalar and Cavusli 2019, Karalar and Cavusli 2020). As seen from these studies, many investigators have examined earthquake behaviour of the rockfill dams in the past. However, the effects of far-fault earthquakes on 3D nonlinear seismic settlement and shear strain behaviour of earth-fill dams were not investigated by researchers. For this reason, this study presents important information related to the nonlinear seismic behaviour and modelling of earth-fill dams. In this study, 3D nonlinear earthquake damage performance of an earth-fill (EF) dam is evaluated under various far-fault ground motions. For this purpose, Oroville EF dam was constructed in United States of America-California in 1968 is selected for three dimensional (3D) finite difference analyses. For seismic analyses, the free field and quiet (viscous) seismic boundary conditions are considered for main surfaces of 3D model of the dam. In the literature, it has been observed that these non-reflective boundary conditions are not frequently used in nonlinear earthquake analysis of EF dams. For this reason, the most important purpose of this study and difference of this study from literature is to evaluate the nonlinear effects of these boundary conditions on the seismic settlement, shear failure and swilling damage behaviour of EF dams. Another aim of this study and another difference of this study from literature is to examine the effects of various far-fault

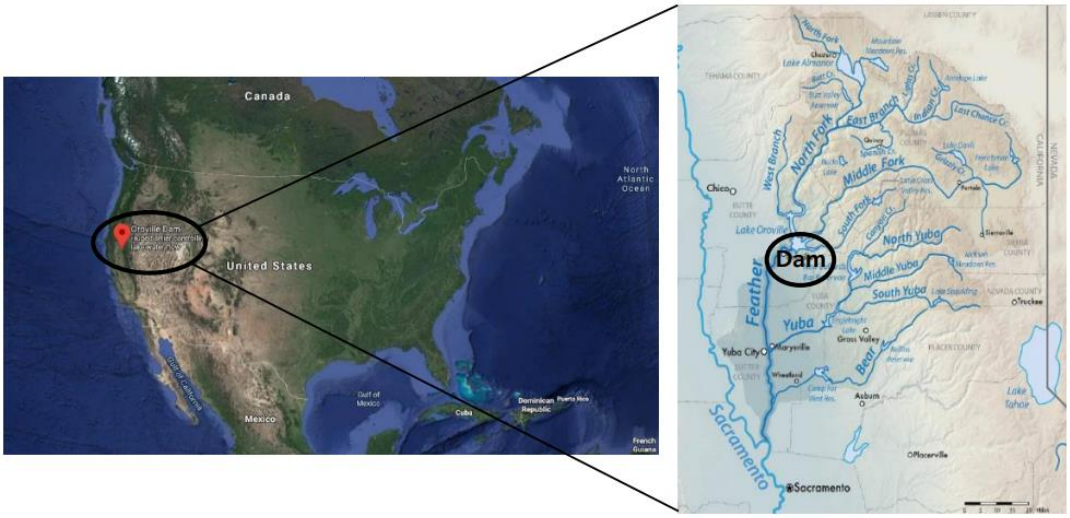

Fig. 1 Map of the Oroville dam, Feather River and its tributaries (Koskinas 2017, Kulhawy and Duncan 1972, Vrymoed 1981)

earthquakes on the nonlinear vertical displacement, shear strain and swilling behaviour of EF dams. For this aim, total 6 different far-fault ground motions are taken into account in the seismic analyses for 234 m (full water level) of reservoir water height. These far-fault earthquakes are 2000 Italy earthquake, 1995 Kobe earthquake, 1984 Morgan Hill earthquake, 1999 Kocaeli earthquake, 1941 Northwest California earthquake, and 1971 San Fernando earthquake, respectively. According to seismic analysis results, it is clearly observed that each far-fault earthquake has dissimilar and important seismic effects on the nonlinear seismic damage performance of Oroville dam body.

2. Oroville Earth-Fill Dam

The Oroville Dam is a 234.7 m (770 ft.) tall earth-fill dam and it was built in 1968. It is the tallest dam in the United States of America and the fifth tallest earth-fill dam in the world (Koskinas 2017, Kulhawy and Duncan 1972, Vrymoed 1981). It is located on the foothills of the Sierra Nevada, on the Feather River, in Butte County, California. Oroville dam and Oroville lake is located in the Feather River (Fig. 1). According to Fig. 1, Feather River is in the south, near Marysville and Yuba City. The Yuba River flows into the Feather River, which in turn flows into the Sacramento River (Koskinas 2017). It leads up to the city of Sacramento, and it finally spills into the Pacific Ocean near the San Francisco Bay (Fig. 1).

Directly below the dam, on the banks of the Feather River where it flows into the base of the Sacramento Valley, lies Oroville, a city of approximately 20000 residents. The name Oroville derives from the Spanish term “Oro” which means gold, and “Ville”, which indicates a city (Koskinas 2017). Originally called Ophir City, it gained this new identity after gold was discovered at Bidwell’s Bar in 1848, near the center of what is now Lake Oroville (Koskinas 2017, Kulhawy and Duncan 1972, Vrymoed 1981). This location was one the first gold mining camps in California, but was quickly depleted of its resources during a mining rush in the years 1856 to 1857. Following these events, the miners abandoned Bidwell’s Bar and moved to Oroville. The entire area was subsequently flooded in 1968 upon the completion of Oroville Dam’s construction (Koskinas 2017, Kulhawy and Duncan 1972, Vrymoed 1981).

Oroville Dam is a zoned earth-fill embankment structure with a maximum height of 235 m (770ft.) above streambed excavation. The embankment itself has a volume of approximately 61 million m^3 (80 million cubic yards) and is comprised of an inclined impervious core atop a concrete foundation, supplemented by zoned earth-fill sections on both sides (Koskinas 2017). Oroville Dam’s spillway, located on the right abutment of the main dam, is comprised of two independent elements: a gated flood control outlet and an uncontrolled emergency spillway. The former consists of an unlined approach channel, a gated headwork, and a lined chute approximately 930 m (3050 ft.) in length, extending down to the Feather River (Koskinas 2017, Kulhawy and Duncan 1972, Vrymoed 1981). The latter is an ungated concrete ogee weir with the crest set at elevation 274.62 m (901 ft.), just one foot above maximum storage level (elevation 274.32 m or 900 ft.). The area below the emergency spillway is not lined with concrete, meaning that when it is put to use, flow will spill over natural terrain. Most of the streamflow released from Lake Oroville passes through the Edward Hyatt Power plant, located in the dam’s left abutment. Total output of the plant is estimated at 678.75 MW, produced by 6 Francis-type turbines, rated at approximately 115 MW each (Koskinas 2017). It is also capable of pump-storage, which offers the potential to maximize the value of generated energy. This station is underground, with dimensions of approximately 168 m by 21 m by 43 m (550 feet long, 69 feet wide, 140 feet high). The intake for the Hyatt Power plant is a sloping concrete structure, built just upstream of the Oroville Dam’s left abutment. It is comprised of two parallel channels, one for each of the two 6.7 m (22 ft.) diameter penstock tunnels. The openings of the intake are protected from incoming debris by steel trash racks. Beneath the trash racks, a square shutter system 12.2 m (40 ft.) wide determines the level and

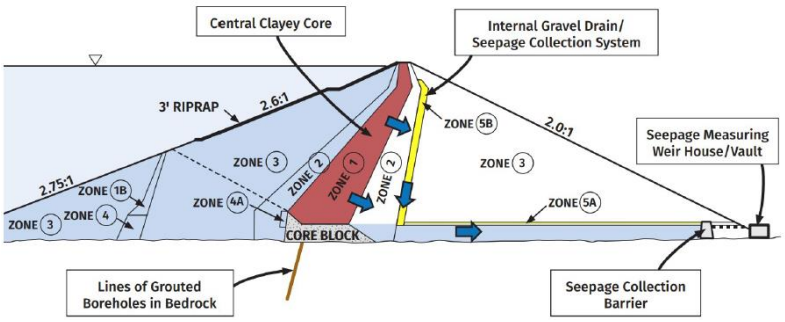

Fig. 2 Cross section of Oroville Dam (Koskinas 2017, Kulhawy and Duncan 1972, Vrymoed 1981)

Table 1 Material properties of Oroville Dam body (Koskinas 2017, Kulhawy and Duncan 1972, Vrymoed 1981, Hydraulic Model Studies of the Flood Control Outlet and Spillway for Oroville Dam California, Department of Water Resources State of California (Report No. Hyd-510) 1965)

Characteristics	SpecificWeight	MaximumUnit Weight	Porosity	Water Content	Air Content	Material Content	Friction Angle	Cohesion	Poisson's Ratio
Unit	g/cm^3	g/cm^3	%	%	%	%	(º)	(kPa)	-
Zone 1	2.47	1.59	26.45	7.40	14.95	63.55	42	0	0.32
Zone 2	2.52	1.69	27.46	7.59	16.57	76.84	45	0	0.35
Zone 3	2.64	2.03	22.91	5.05	12.56	78.39	47	0	0.34
Zone 4	2.88	1.82	24.15	8.78	16.97	71.25	46	0	0.33
Zone 5	3.17	2.17	24.35	5.50	16.75	71.78	49	0	0.31
Foundation	3.07	2.05	25.48	7.78	17.87	76.26	52	0	0.25

Fig. 3 Aerial view of Oroville dam (California-America) (Koskinas 2017, Kulhawy and Duncan 1972, Vrymoed 1981, Hydraulic Model Studies of the Flood Control Outlet and Spillway for Oroville Dam California, Department of Water Resources State of California (Report No. Hyd-510) 1965)

temperature of the water withdrawn from the reservoir (Koskinas 2017). Especially the temperature of the water withdrawn can be critical for local agricultural purposes, as well as for the local wildlife. In addition, in case of an emergency, the penstocks can be closed through hydraulically activated gates located at the base of the intake channels. However, under standard operation conditions, any discharges from the Hyatt Power plant are conveyed to the Feather River with the use of the dam's two former diversion tunnels, each 10.7 m (35 ft.) in diameter. In the event of a prolonged outage at the plant, water flows directly through these into a downstream river outlet, with a maximum release of 151.2 m^3/s (5,400 cfs) (Koskinas 2017, Kulhawy and Duncan 1972, Vrymoed 1981). Cross section of Oroville Dam, including seepage barriers and the seepage collection system is shown is Fig. 2. Moreover, aerial view of Oroville dam is shown in Fig. 3.

Materials that were used in Oroville dam's body are explained as below:

Zones 1, 1A, 1B: Impervious core from the deposit next to the pervious borrow areas. A well-graded mixture of silt, sand, gravels, and cobbles up to 180 mm in diameter.

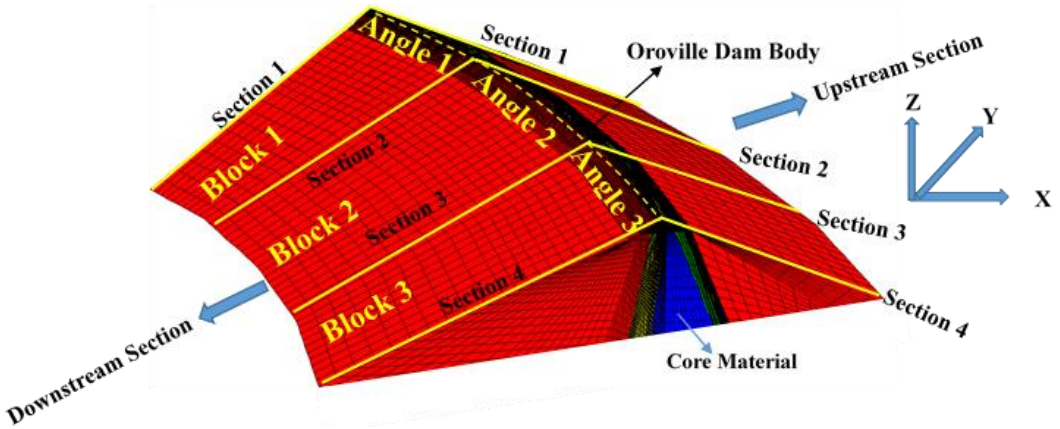

Fig. 4 Three dimensional blocks and sections in the Oroville EF dam body

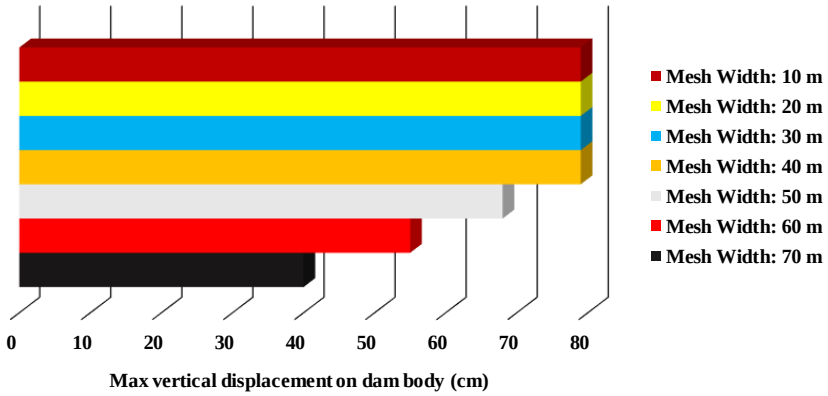

Fig. 5 Vertical displacement changes on the crest for different mesh widths

Compacted in 25.4 cm (10 inch) lifts by 100-ton pneumatic rollers (Koskinas 2017, Kulhawy and Duncan 1972, Vrymoed 1981).

Zone 2: Transition zone comprised of a well-graded mixture of silt, sand, gravels, cobbles, and boulders up to 380 mm in diameter. Compacted in 38 cm (15-inch) lifts by a smooth-drum vibratory roller (Koskinas 2017, Kulhawy and Duncan 1972, Vrymoed 1981).

Zone 3: Shell zone, comprised of mostly sands, gravels, cobbles, and boulders up to 610 mm in size. Compacted in 61 cm (24-inch) lifts by a smooth-drum vibratory roller (Koskinas 2017, Kulhawy and Duncan 1972, Vrymoed 1981). Zone 4: Impervious core containing selected abutment stripping, between 15 and 45 percent passing standard No. 200 US Standard sieve with 200 mm maximum size. Compacted in 25.4 cm (10 inch) lifts by 100-ton pneumatic rollers (Koskinas 2017, Kulhawy and Duncan 1972, Vrymoed 1981).

Zones 5A, 5B: Drainage zones built out of gravels, cobbles, and boulders. Maximum of 12 percent larger than No.4 sieve size permitted. Compacted in 61 cm (24-inch) lifts by a smooth-drum vibratory roller (Koskinas 2017, Kulhawy and Duncan 1972, Vrymoed 1981).

Material properties of Oroville EF Dam body are shown in Table 1.

3. 3D modelling and calibrating of Oroville EF dam

3D modelling and investigating of the seismicity of earth-fill (EF) dams such as Oroville EF dam is vital importance to evaluate the future and safety of such dams. In this section, important information about the modelling of Oroville dam is explained in detail. Because of Oroville dam is one of the biggest water structures in the world, examining and modelling seismicity of this dam provide significant contributions to the literature. Oroville dam has not got a flat dam body as other Earth-fill dams. It has an oval body structure and this oval geometry has three different angles (Fig. 4). Firstly, the foundation of 3D finite difference model is modelled taking into account the geological structure of the canyon. While modelling the foundation, the height of the foundation is considered as the height of the dam body. Moreover, the foundation is extended towards the dam body's right and left directions as the height of the dam body. The location and geometry of each material in the dam body are different from each other. While creating the geometry of the dam body, 3D model of all materials is modelled in accordance with the original dam project. In addition, the height of the dam body is modelled in accordance with the elevation of the rough terrain. The dam body has 3 different blocks and 4 different sections. These blocks and sections in the dam body are shown in Fig. 4 in detail. Totally, there are 3961591 nodal points in the 3D model of Oroville Dam. Mesh ranges are not randomly created in the 3D model. The most stable mesh range is taken into account in this study as seen in Fig. 5. In order to find correct mesh width, total of 7

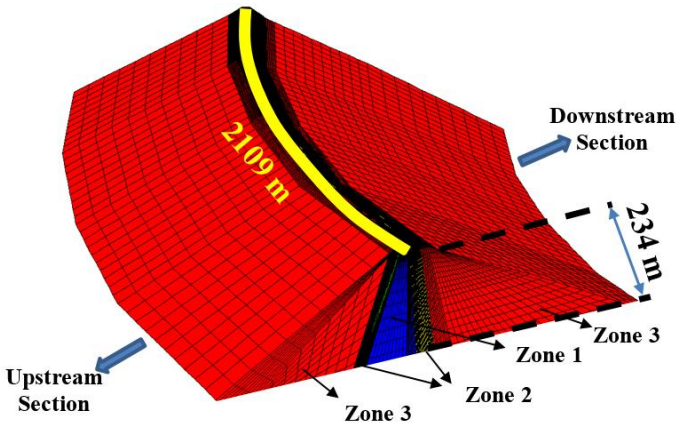

Fig. 6 Specific view of materials in 3D model of Oroville EF dam

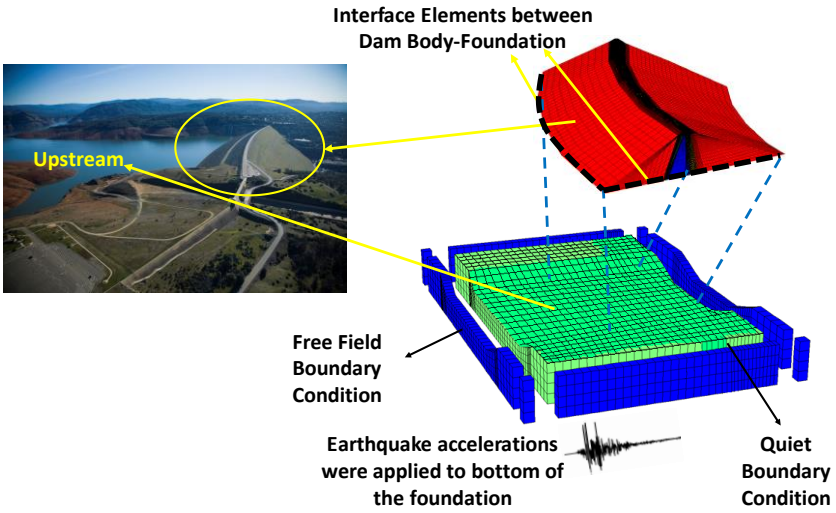

Fig. 7 Free field and quiet boundary conditions for 3D model of Oroville dam

different mesh widths are created and stability analyses are performed for these mesh width.

These widths are 10 m, 20 m, 30 m, 40 m, 50 m, 60 m, 70 m, respectively (Karalar and Cavusli 2019). It is seen from numerical analyses that the maximum settlements on the crest of the dam do not change for less mesh width than 40 m (Fig. 5). Thus, mesh width is selected approximately 40 m for seismic analyses. Locations of each material are different in the dam body and these materials are shown in detail in Fig. 6.

Moreover, special interface elements are used between the dam body and foundation to represent the interaction condition of discrete surfaces in this study. Normal (k_n) and shear (k_s) interaction stiffness values are different for each interface surface. Unit of the k_n and k_s stiffness is stress/displacement (Itasca 2002). In this study, k_n and k_s stiffness are separately calculated for each discrete surface (Karalar and Cavusli 2019). These stiffness values are considered as approximately 10^8 Pa/m between the dam body and foundation (Karalar and Cavusli 2019). Shear and normal stiffness values are defined to FLAC3D software using special fish functions (Karalar and Cavusli 2019). The reservoir water is modelled considering the hydrostatic pressure and leakage in the dam body. All surfaces exposed to the hydrostatic pressure are separately grouped in the 3D model to apply hydrostatic water pressure to these surfaces. Hydrostatic water loads were applied from the crest to the foundation surface. These water loads are contacted to each node. In order to obtain the water leakage, a water table was applied to the upstream part of the dam taking into account the maximum water height (234 m). Hydrostatic water loads and water tables are defined to FLAC3D software using special fish functions (Karalar and Cavusli 2019). Free field and quiet (viscous) boundary conditions are applied only lateral surfaces of the 3D model. Firstly, free field special seismic boundary condition is defined to software using special fish functions. Afterwards, the quiet boundary condition is considered to lateral surfaces of the 3D model. These special seismic boundary conditions are shown in Fig. 7. Total 6 various far-fault ground motions are used in this study. These earthquakes are practiced to the bottom of the foundation to represent the reality of the damage analysis as seen in Fig. 7.

4. Three dimensional nonlinear seismic analysis results

When examined the literature, it is clearly seen that

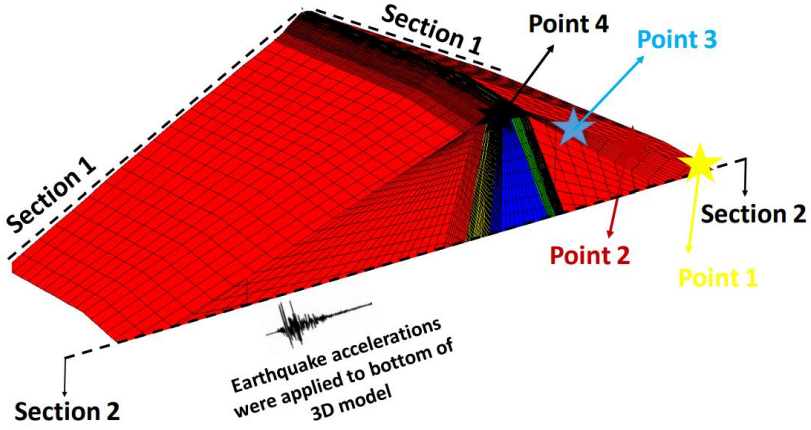

Fig. 8 View of four nodal points on the dam body surface

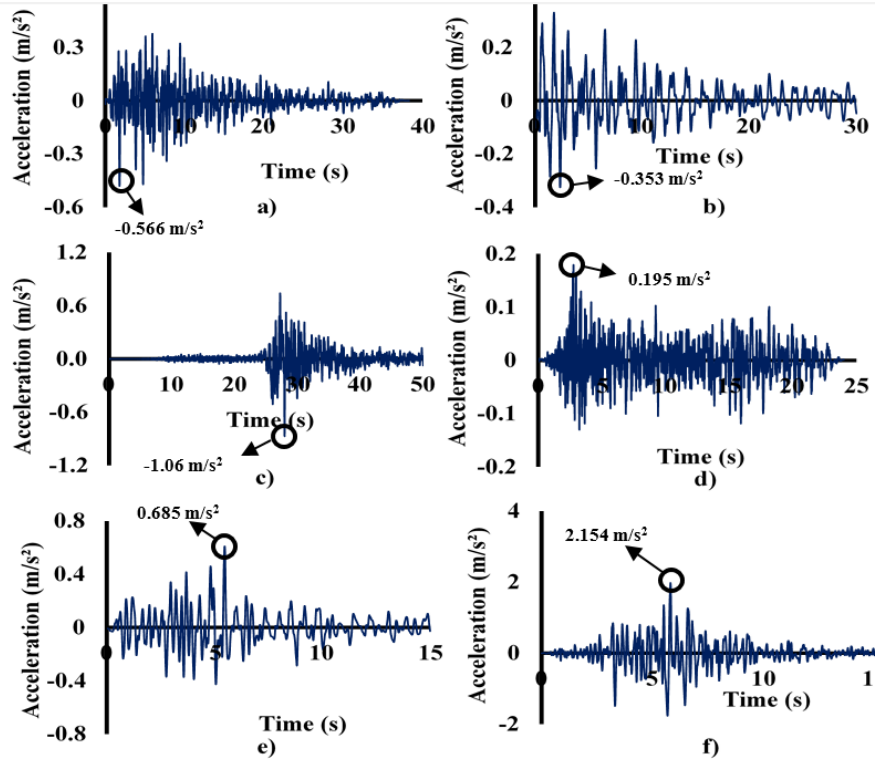

Fig. 9 Acceleration-time graphics for; (a) 2000 Italy earthquake, (b) 1995 Kobe earthquake, (c) 1999 Kocaeli earthquake (d) 1984 Morgan Hill earthquake, (e) 1941 Northwest California earthquake and (f) 1971 San Fernando earthquake (PEER 2010)

there is no study related to the effects of far-fault ground motions on the seismic settlement and shear strain behaviour of earth-fill dams in the literature. In order to fill these deficiencies, nonlinear far-fault earthquake behaviour of Oroville earth-fill dam is examined considering different far-fault earthquakes in this study. The nonlinear seismic behaviour of Oroville dam is graphically investigated considering 6 important far-fault ground motions. Moreover, four nodal points are selected from the dam body surface to better see changing of nonlinear seismic behaviour of the dam. These points are shown in Fig. 8 in detail. In the numerical analysis results, Point 1 and 2 are shown as yellow colour and red colour, respectively. In addition, Point 3 is blue colour and Point 4 is shown as black colour in the graphics.

In the seismic analysis results, deformations, vertical displacements and shear strain failures are graphically presented and assessed for four nodal points on the dam body surface. Besides, these numerical results are compared as graphically and contour plot diagram for various far-fault ground motions. In the seismic analyses, duration of the 2000 Italy earthquake is 40 seconds and 1995 Kobe earthquake is 30 seconds. For the Kocaeli and 1984 Morgan Hill earthquakes, duration is 50 and 25 seconds, respectively. Finally, 1971 San Fernando and 1941 Northwest California earthquakes are 15 seconds. These earthquakes have different magnitudes and accelerogram. In addition, these earthquakes have different time intervals

Table 2 Characteristic properties of far fault earthquakes (PEER 2010)

Earthquake	Distance (km)	PGA (g)	PGV (cm/s)	Duration (s)
2000 Italy earthquake	60	0.142	12.9	40
1995 Kobe earthquake	52	0.139	12.7	30
1999 Kocaeli earthquake	66	0.169	13.7	50
1984 Morgan Hill earthquake	82	0.132	11.8	25
1941 Northwest California earthquake	74	0.155	13.2	15
1971 San Fernando earthquake	69	0.198	14.7	15

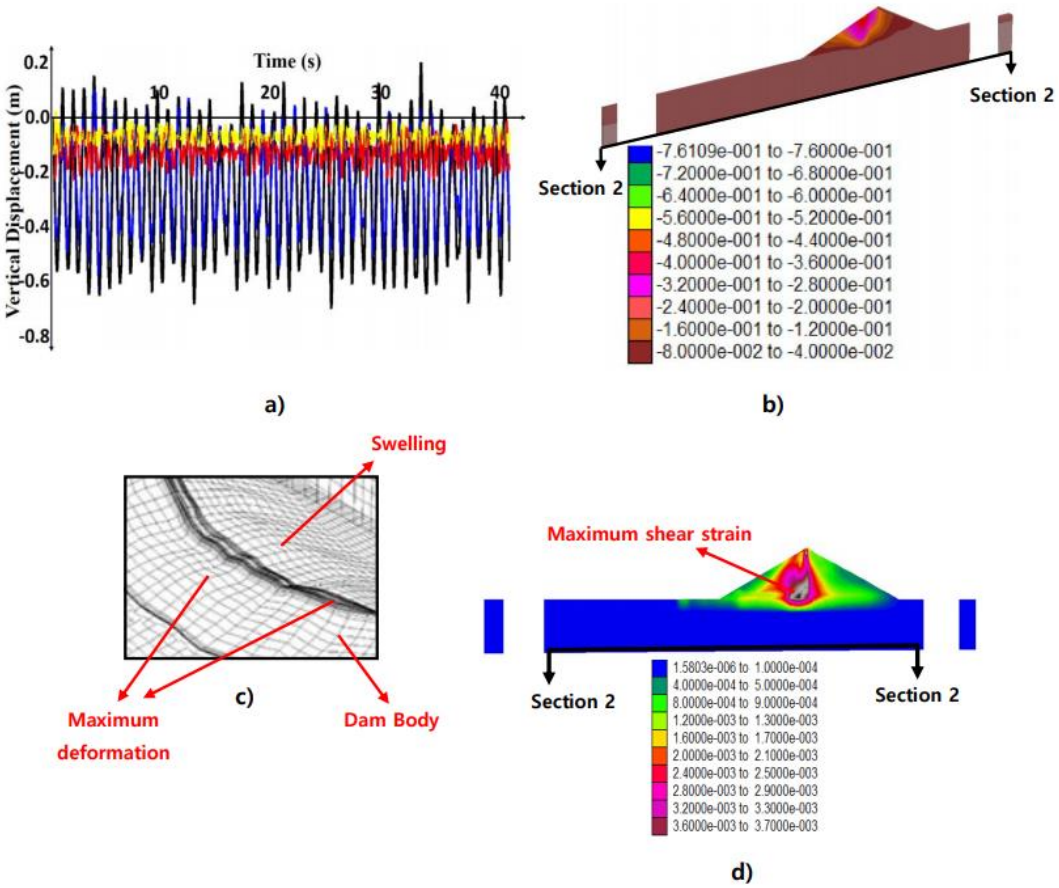

Fig. 10 Seismic analysis results for 2000 Italy earthquake; (a) Time-history graphic, (b) Contour diagram for max vertical displacement on dam at 40th second of earthquake, (c) Deformation behaviour of dam body at 40th second of earthquake and (d) 2D contour diagram for max shear strain in dam at 40th second of earthquake

from each other. Acceleration-time graphics of the far-fault earthquakes are presented in Fig. 9. Besides, characteristic properties of far fault earthquakes are shown in Table 2.

For EF dams that were constructed on the seismic zones, significant vertical displacements and shear strains may occur in the dam body by the effects of far-fault earthquake loads and hydrostatic pressure. In this section, vertical displacement and shear strain results of Oroville EF dam are assessed under 6 various far-fault ground motions (Fig. 10-15). In Fig. 10, nonlinear vertical displacement and shear strain results are shown for 2000 Italy far-fault earthquake. According to Fig. 10a, maximum vertical displacement is observed on the Point 4 (top point) and its numerical value is -0.75 m. -0.75 m is very critical for safety and future of EF dams. When Point 4 and Point 3 is compared with each other, less settlement values are obtained for Point 3. In addition, minimum vertical displacement is acquired on Point 1 and more settlement values occurred on the Point 2 as compared with Point 1. Positive settlements are observed on Point 4 during the earthquake. When considered this maximum displacement (-0.75 m), it is clearly understood that far-fault ground motions have vital important nonlinear seismic settlement effects on the earthquake behaviour of EF dams. In Fig. 10b, settlement contour plot diagram is shown for non-reflecting boundary condition. The maximum settlement is -0.76 m at 40th second of the earthquake and it occurred on the top sections of the dam body. Moreover, settlements increased from crest point to foundation and there is no significant settlement on the foundation surface. In Fig.

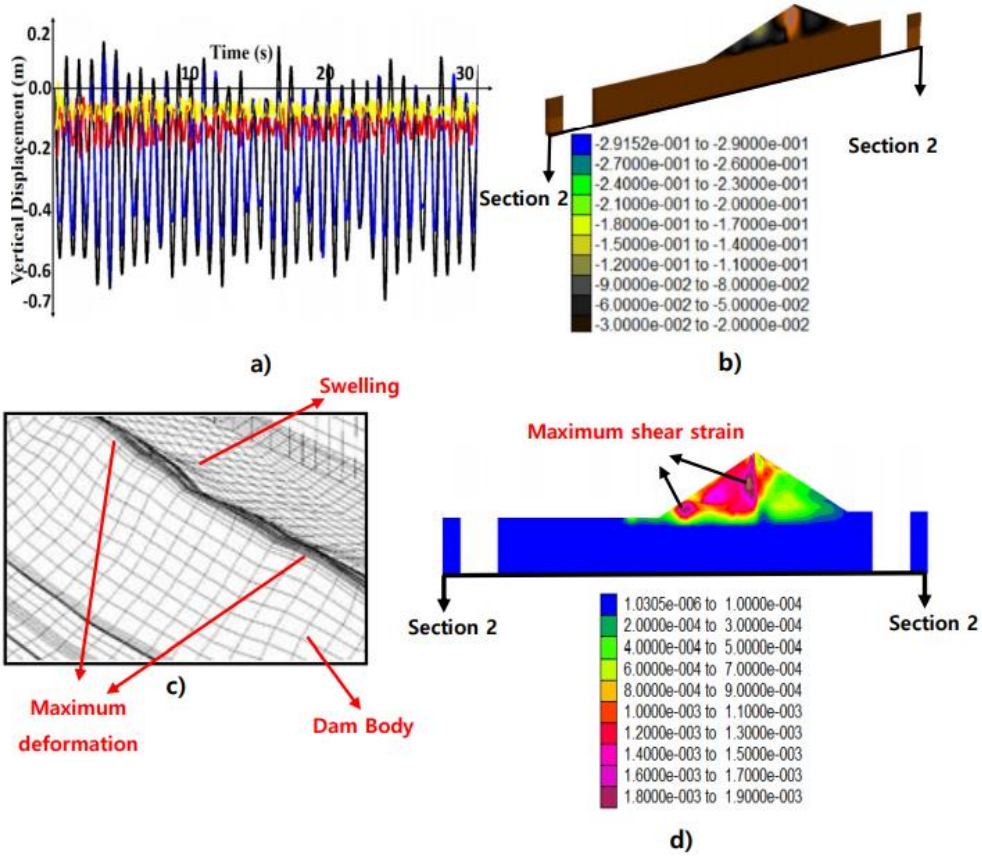

Fig. 11 Seismic analysis results for 1995 Kobe earthquake; (a) Time-history graphic, (b) Contour diagram for max vertical displacement on dam at 30th second of earthquake, (c) Deformation behaviour of dam at 30th second of earthquake and (d) 2D contour diagram for max shear strain in dam at 30th second of earthquake

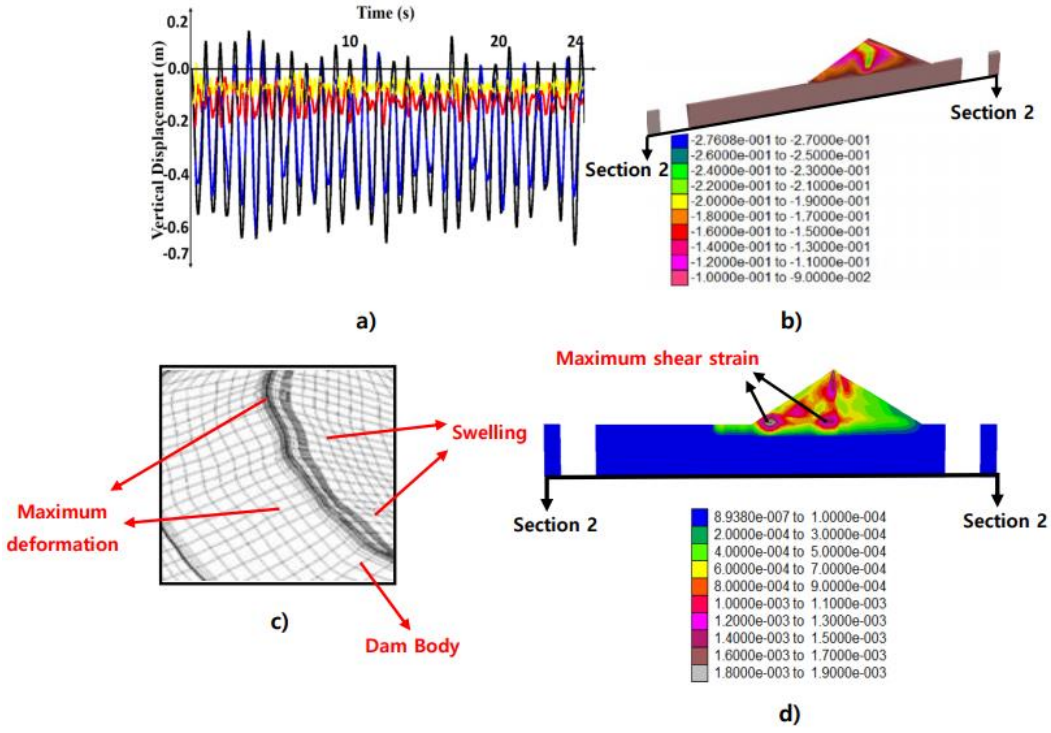

Fig. 12 Seismic analysis results for 1984 Morgan Hill earthquake; (a) Time-history graphic, (b) Contour diagram for max vertical displacement on dam at 24th second of earthquake, (c) Deformation behaviour of dam at 24th second of earthquake and (d) 2D contour diagram for max shear strain in dam at 24th second of earthquake

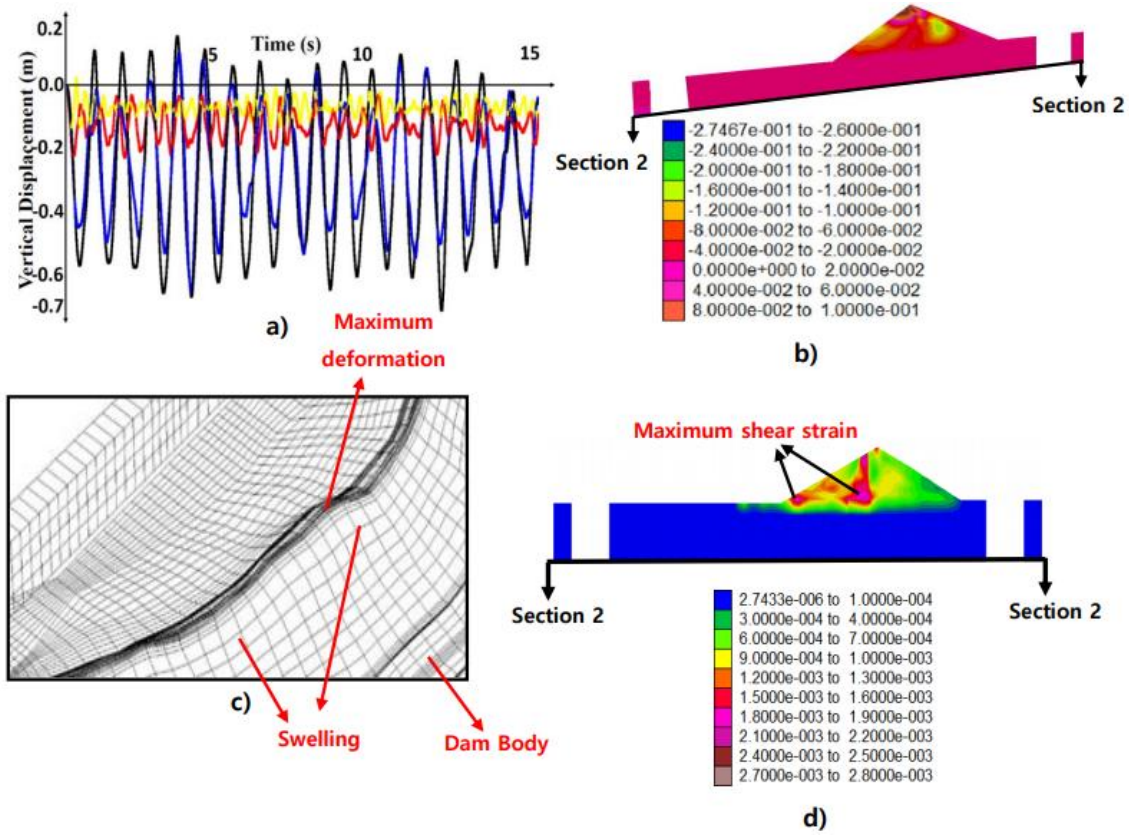

Fig. 13 Seismic analysis results for 1941 Northwest California earthquake; (a) Time-history graphic, (b) Contour diagram for max vertical displacement on dam at 15th second of earthquake, (c) Deformation behaviour of dam at 15th second of earthquake and (d) 2D contour diagram for max shear strain in dam at 15th second of earthquake

10(c), deformation behaviour of Oroville EF dam at 40th second of the earthquake is shown in detail. According to Fig. 10(c), it is clearly observed that Italy far-fault earthquake strongly affected the deformation behaviour of the dam body and these seismic deformations are very significant for EF dams. Maximum deformation on the dam body occurred at middle section of the dam body (Fig. 10(c)). Although no significant deformations occurred on the foundation during the earthquake, significant deformations are observed on the dam body by effects of the far-fault earthquake. In Fig. 10(d), shear strain behaviour of Oroville EF dam is presented in detail. According to Fig. 10(d), it is obviously seen that maximum shear strain failure occurred in the core and this information is very important to evaluate shear strain behaviour of EF dams. It is clearly observed that far-fault earthquakes may cause significant shear stresses in the EF dam body.

In Fig. 11, nonlinear settlement and shear strain behaviour of Oroville dam is presented for the 1995 Kobe far-fault earthquake. According to Fig. 11(a), seismic settlements are graphically shown for four nodal points. During the earthquake, maximum settlement is -0.72 m and this significant value occurred on the Point 4. -0.72 m vertical displacement may give rise to very important safety problems for EF dams. Thus, while modelling a EF dam, far-fault earthquakes should not be ignored in the seismic analyses. In addition, minimum settlement is observed on Point 1. As compared Point 2 and Point 3, more settlements are obtained for Point 3. In Fig. 11(b), 3D settlement contour plot diagram is presented for 2-2 section (the most critical section) of the dam body. -0.29 m maximum settlement occurred at top sections of the dam body for 30th second of the earthquake. There are no significant settlements on the foundation surface and significant vertical displacements are observed at this second. Moreover, there are no important settlements on cofferdam section of the dam at last section of the earthquake. In Fig. 11(c), nonlinear deformation behaviour of Oroville dam is shown in detail. According to Fig. 11(c), maximum deformations are observed on the middle section of the dam body surface and significant swellings occurred on the downstream surface of dam body. This situation is evidence of the effects of hydrostatic pressure and far-fault earthquake loads. When examined Fig. 11(d), far fault seismic shear strain behaviour of Oroville dam is clearly seen and it is obviously observed that maximum seismic shear strains occur at core of the dam body during far fault earthquake. This result is very important for modelling and analysing of seismic behaviour of EF dams.

In Fig. 12, vertical displacement and shear strain results for 1984 Morgan Hill far-fault earthquake are presented as graphically and contour plot diagram. According to Fig. 12(a), the maximum settlement is observed on the Point 4 (top point), and its numerical value is -0.70 m. Minimum vertical displacement is obtained at the Point 1. Although, close vertical displacement is acquired for Points 1 and 2

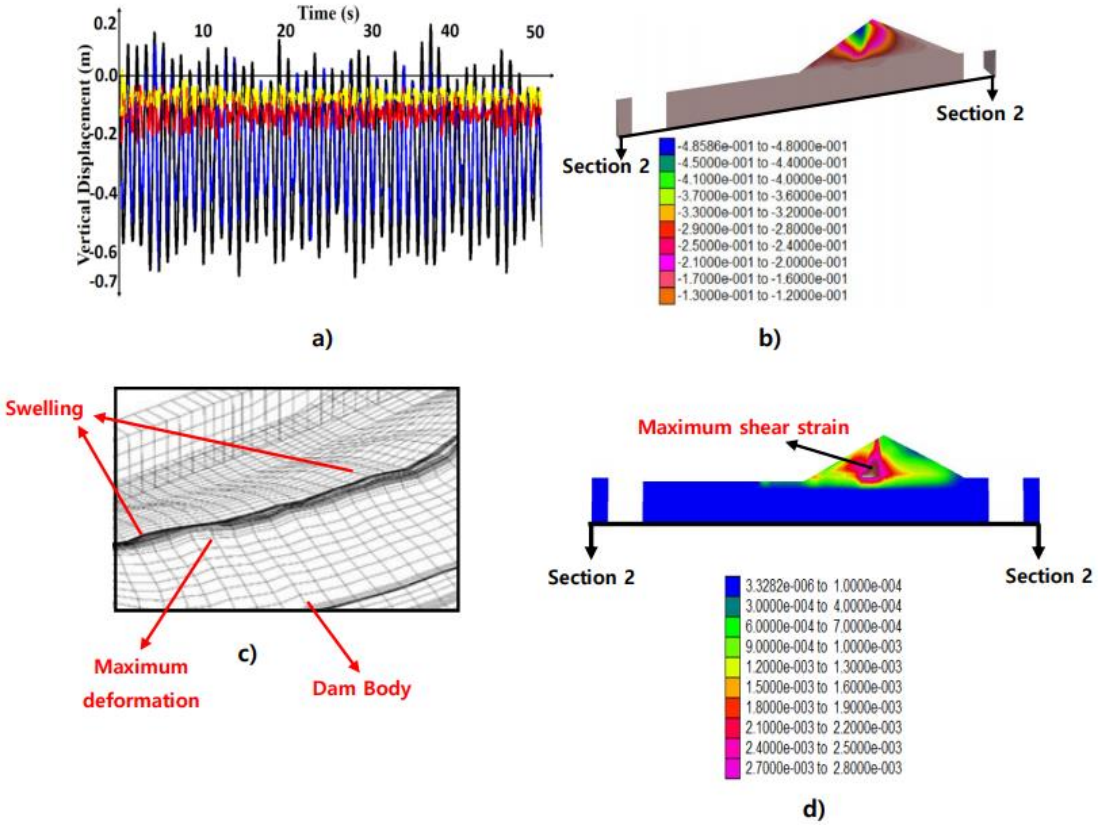

Fig. 14 Seismic analysis results for 1999 Kocaeli earthquake; (a) Time-history graphic, (b) Contour diagram for max vertical displacement on dam at 50th second of earthquake, (c) Deformation behaviour of dam at 50th second of earthquake and (d) 2D contour diagram for max shear strain in dam at 50th second of earthquake

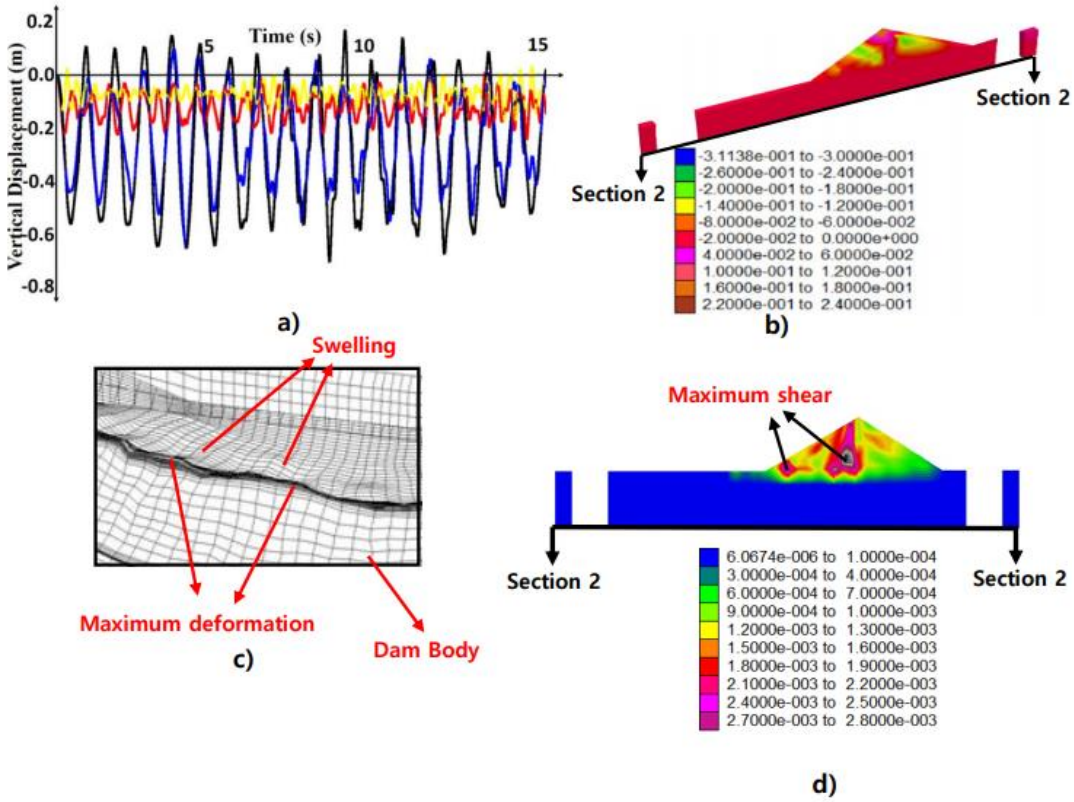

Fig. 15 Seismic analysis results for 1971 San Fernando earthquake; (a) Time-history graphic, (b) Contour diagram for max vertical displacement on dam at 15th second of earthquake, (c) Deformation behaviour of dam at 15th second of earthquake and (d) 2D contour diagram for max shear strain in dam at 15th second of earthquake

during the earthquake, more settlements are observed for Point 2 as compared with Point 1. In Fig. 12(b), 2D contour plot diagram is shown considering 2-2 section of the dam body. -0.276 m maximum settlement is obtained on the top sections of the dam body. Moreover, far-fault earthquake did not significantly affect the foundation of the dam. According to Fig. 12c, nonlinear deformation behaviour of Oroville dam is observed in detail. As seen from Fig. 12(c), far-fault earthquake strongly affected seismic behaviour of the dam body and maximum deformations are observed on the middle section of the dam body surface. In Fig. 12(d), two dimensional shear strain behaviour of Oroville dam is examined taking into account 2-2 section of the dam. Maximum shear stresses are observed at core and minimum shear strains occurred at foundation. Moreover, significant shear failures are also obtained at core of cofferdam. This result proves that maximum shear strains occur around the core during the earthquake.

In Fig. 13, nonlinear seismic settlement behaviour of Oroville EF dam is presented for 1941 Northwest California far-fault earthquake. When examined Fig. 13(a), it is clearly seen the seismic effects of far-fault earthquake on the vertical displacement behaviour of the EF dams. -0.74 m maximum settlement is observed on the Point 4 (top point) at the 12.1th second of the earthquake. -0.74 m vertical displacement is very significant seismic problem for EF dams. Thus, it is clearly indicated that examination of effects of far-fault earthquakes on the seismic behaviour of EF dams is very important for safety and future these dams. Minimum settlements are obtained on Point 1 and as compared Points 1 and 2, more vertical displacements are observed on the Point 2. In Fig. 13(b), 3D settlement contour plot diagram is shown for non-reflecting boundary condition. -0.27 m maximum settlement is acquired on the top sections of the dam. In addition, 0.1 m maximum positive settlement is observed in the dam body at the 15th second of the earthquake. According to Fig. 13(c), deformation behaviour of the dam is shown in detail. As seen from Fig. 13(c), significant deformations occurred on dam body surface at 15th second of the earthquake. Deformations may cause important safety problems and prediction of possible seismic deformations for EF dams has great importance in the structural engineering problems. Therefore, Fig. 13(c) helps to researchers to get an idea about this engineering problem. As examined Fig. 13(d), it is clearly seen that maximum shear strains occurred around core and this result is very importance for EF dams. Moreover, minimum shear strains are observed at the foundation.

In Fig. 14, numerical settlement and shear failure results are shown for the 1999 Kocaeli far-fault earthquake. According to Fig. 14(a), -0.69 m maximum vertical displacement is obtained on the Point 4 and minimum settlement is observed on the Point 1. -0.69 m vertical displacements may give rise to important safety problems for EF dams. So, importance of far-fault earthquakes for the nonlinear seismic behaviour of EF dams is proved with this numerical result. In addition, when compared Points 2 and 3, more vertical displacements are acquired for Point 3. In Fig. 14(b), 3D settlement contour plot diagram is presented for full reservoir condition. Hydrostatic pressure effects on the dam body are clearly seen from Fig. 14(b). -0.48 m maximum settlement is observed on the dam body surface at 50th second of the earthquake. There are no significant vertical displacements on the foundation surface during the earthquake. When examined Fig. 14(c), it is clearly seen the effects of far-fault earthquakes on the deformation behaviour of Oroville dam. Significant deformations are observed on the dam body surface and these deformations may cause important safety problems for EF dams. Important swellings occurred at downstream side of the dam body (Fig. 14(c)). According to Fig. 14(d), shear failure behaviour of Oroville EF dam is shown in detail. Maximum failure occurred at core and minimum shear failure is observed at foundation. This result is shown that the most critical material for seismic safety of EF dams is core and maximum failure occur in this material.

In Fig 15, nonlinear vertical displacement and shear strain results are shown as graphically and contour plot diagram for the 1971 San Fernando earthquake. According to Fig. 15(a), -0.75 m maximum settlement is observed on the Point 4, and minimum settlement is obtained on the Point 1. As compared Points 3 and 4, less vertical displacements are acquired for Point 3. In Fig. 15(b), contour plot diagram is presented for non-reflecting boundary condition. -0.31 m maximum settlement is obtained on the dam body surface at the 15th second of the earthquake. Moreover, +0.24 m maximum positive settlement is acquired in the dam body at this second. No significant settlements are observed on the foundation surface. In Fig. 15(c), seismic deformation behaviour of Oroville dam is examined in detail. Maximum deformations are observed at middle section of the dam body surface and these deformations are vital important for safety of the EF dams. Significant swellings are obtained at last section of the earthquake and these swellings are observed at downstream section of the dam. According to Fig. 15(d), 2D shear failure behaviour of Oroville dam is shown as graphically. It is clearly seen that maximum failures are observed at core of the dam and cofferdam. This result proves that maximum failures occur at core for EF dams and far-fault earthquakes mostly affect core during the earthquake. When these results are examined in detail, it is clearly seen that there are different shear strains in the dam body for various far fault earthquakes. The only reason for this result is that different far fault earthquakes create different seismic effects in the dam body, and since each far earthquake have different characteristic properties and durations, these ground motions differently affect the earthquake behaviour of the dam from each other. However, it is obviously seen that maximum shear strains occurred in core of the dam for six different far fault earthquakes.

5. Conclusions

In this study, nonlinear seismic behaviour of Oroville Earth-Fill (EF) dam is examined under 6 various far-fault ground motions. Three dimensional finite difference model of the Oroville dam is created according to the original dam project. While modelling the dam, non-reflecting seismic boundary conditions were rarely used for 3D seismic

analyses of EF dams in the past are used for Oroville EF dam. In addition, Mohr-Coulomb nonlinear material model is utilized for the dam materials and foundation. In the nonlinear seismic analyses, far-fault earthquake accelerations are applied to the bottom of the 3D model using special fish functions. According to earthquake analyses, nonlinear seismic effects of far-fault earthquakes on deformation and shear failure behaviour of Oroville EF dam are examined in detail and these numerical results are evaluated as below:

• In the literature, far-fault earthquakes were not considered for modelling or analysing of EF dams. However, it is clearly revealed in this study that far-fault earthquakes have significant seismic effects on the nonlinear earthquake behaviour of EF dams. Thus, it is strongly proposed that far-fault earthquakes should be taken into account for seismic modelling and analysing of a EF dam.

• The non-reflecting boundary condition (free field and quiet) were used in this study represents an existing situation in nature. Thus, it is clearly proposed that this boundary condition is a new seismic boundary condition for analysing of EF dams should be used in the seismic analyses of EF dams to obtain more safety seismic numerical results.

• When examined settlement analysis results, maximum vertical displacements are observed at top sections of the dam body, and minimum settlements are obtained on lowest sections of the dam body. According to all earthquake analyses, approximately 75 cm maximum settlement is obtained during the earthquakes and obtained settlement result may give rise to important seismic safety problems for EF dams. Thus, importance of far-fault earthquakes on the nonlinear seismic settlement behaviour of EF dams is clearly understood with this numerical result.

• According to seismic analysis results, significant deformations are observed at last section of the far-fault earthquakes. Maximum deformations occurred on middle sections of the dam body surface. Moreover, significant swellings are observed at downstream section of the dam body surface. These deformations and swellings are vital for safety and future of EF dams. Thus, in this study, it is clearly proposed that far-fault earthquakes should not be ignored in analysing of deformation behaviour of EF dams.

• When shear strain results are evaluated, it is obviously indicated that during far-fault earthquakes, significant shear failures may occur in dam body. Maximum shear failures are obtained in the core and important shear failures are also acquired in the core of the cofferdam. These results clearly prove that the most critical material for seismic behaviour of EF dams is core.

References

Akpınar, U., Binici, B. and Arıcı, Y. (2014), "Earthquake stresses and effective damping in concrete gravity dams", *Earthq. Struct.*, **6**(3), 251-266. http://doi.org/10.12989/eas.2014.6.3.251.

Albano, M., Modoni, G., Croce, P. and Russo, G. (2015), "Assessment of the seismic performance of a bituminous faced Earth-fill dam", *Soil Dyn. Earthq. Eng.*, **75**, 183-198. https://doi.org/10.1016/j.soildyn.2015.04.005.

Arefian, A., Noorzad, A., Ghaemian, M. and Hosseini, A. (2016), "Seismic evaluation of cemented material dams-A case study of Tobetsu Dam in Japan", *Earthq. Struct.*, **10**(3), 717-733. https://doi.org/10.12989/eas.2016.10.3.717.

Cavusli, M. (2016), "Investigation of three dimensional non-linear behaviour of Ataturk Dam", Master Thesis, Zonguldak Bulent Ecevit University, Zonguldak, Turkey.

Cen, W.J., Wen, L.S., Zhang, Z.Q. and Xiong, K. (2016), "Numerical simulation of seismic damage and cracking of concrete slabs of high concrete face Earth-fill dams", *Water Sci. Eng.*, **9**(3), 205-211. https://doi.org/10.1016/j.wse.2016.09.001.

Chen, S.S., Fu, Z.Z., Wei, K.M. and Han, H.Q. (2016), "Seismic responses of high concrete face Earth-fill dams: A case study", *Water Sci. Eng.*, **9**(3), 195-204. https://doi.org/10.1016/j.wse.2016.09.002.

Dakoulas, P. (2012), "Nonlinear seismic response of tall concrete-faced Earth-fill dams in narrow canyons", *Soil Dyn. Earthq. Eng.*, **34**(1), 11-24. https://doi.org/10.1016/j.soildyn.2011.09.004.

Haciefendioglu, K. (2006), "Transient stochastic analysis of nonlinear response of earth and rock-fill dams to spatially varying ground motion", *Struct. Eng. Mech.*, **22**(6), 647-664. https://doi.org/10.12989/sem.2006.22.6.647.

Haciefendioglu, K., Bayraktar, A. and Turker, T. (2010), "Seismic response of concrete gravity dam-ice covered reservoir-foundation interaction systems", *Struct. Eng. Mech.*, **36**(4), 499-511. https://doi.org/10.12989/sem.2010.36.4.499.

Haciefendioglu, K. and Soyluk, K. (2016), "Nonlinear response of earthfill dams to spatially varying ground motion including site response effect", *Adv. Struct. Eng.*, **14**(2), 223-234. https://doi.org/10.1260/1369-4332.14.2.223.

Han, B., Zdravkovic, L., Kontoe, S. and Taborda, D.M.G. (2016), "Numerical investigation of the response of the Yele Earth-fill dam during the 2008 Wenchuan earthquake", *Soil Dyn. Earthq. Eng.*, **88**, 124-142. https://doi.org/10.1016/j.soildyn.2016.06.002.

Hu, H. and Huang, Y. (2019), "A dynamic reliability approach to seismic vulnerability analysis of earth dams", *Geomech. Eng.*, **18**(6), 661-668. https://doi.org/10.12989/gae.2019.18.6.661.

United States Department of the Interior Bureau of Reclamation (1965), "Hydraulic Model Studies of the Flood Control Outlet and Spillway for Oroville Dam California", Report No. Hyd-510, Department of Water Resources State of California, United States Department of the Interior Bureau of Reclamation.

Itasca Consulting Group (2002), FLAC version 5 User Manual, Itcasa Consulting Group, Inc., Minneapolis, U.S.A.

Karalar, M. and Cavusli, M. (2018), "Examination of 3D long-term viscoplastic behaviour of a CFR dam using special material models", *Geomech. Eng.*, **17**(2). https://doi.org/10.12989/gae.2019.17.2.119.

Karalar, M. and Cavusli, M. (2018), "Effect of normal and shear interaction stiffnesses on three-dimensional viscoplastic creep Behaviour of a CFR Dam", *Adv. Civ. Eng.* https://doi.org/10.1155/2018/2491652.

Karalar, M. and Cavusli, M. (2019), "Evaluation of 3D nonlinear earthquake behaviour of the Ilısu CFR dam under far-fault ground motions", *Adv. Civ. Eng.* https://doi.org/10.1155/2019/7358710.

Karalar, M. and Cavusli, M. (2019), "Assessing 3D seismic damage performance of a CFR dam considering various reservoir heights", *Earthq. Struct.*, **16**(2), 221-234. http://doi.org/10.12989/eas.2019.16.2.221.

Karalar, M. and Cavusli, M. (2020), "Seismic effects of epicenter distance of earthquake on 3D damage performance of CG dams", *Earthq. Struct.*, **18**(2), 201-213.

http://doi.org/10.12989/eas.2020.18.2.201.
Kartal, M.E., Cavusli, M. and Genis, M. (2019), "3D nonlinear analysis of Atatürk clay core rockfill dam considering settlement monitoring", *Int. J. Geomech.*, **19**(5), 04019034. https://doi.org/10.1061/(ASCE)GM.1943-5622.0001412.
Koskinas, A.E. (2017), "The Oroville Dam 2017 spillway incident possible causes and solutions", Ph.D. Thesis, National Technical University of Athens, Athens, Greece.
Kulhawy, F.H. and Duncan, J.M. (1972), "Stresses and movements in Oroville Dam", *J. Soil Mech. Found. Div.*, **98**, 653-665.
Lin, P., Huang, B., Li, Q. and Wang, R. (2015), "Hazard and seismic reinforcement analysis for typical large dams following the Wenchuan earthquake", *Eng. Geol.*, **194**, 86-97. https://doi.org/10.1016/j.enggeo.2014.05.011.
Lotfi, V. (2005), "Significance of rigorous fluid-foundation interaction in dynamic analysis of concrete gravity dams", *Struct. Eng. Mech.*, **21**(2), 137-150. https://doi.org/10.12989/sem.2005.21.2.137.
Lotfi, V. (2006), "An efficient three-dimensional fluid hyper-element for dynamic analysis of concrete arch dams", *Struct. Eng. Mech.*, **24**(6), 683-698. https://doi.org/10.12989/sem.2006.24.6.683.
Nimbalkar, S., Annapareddy, V.S.R. and Pain, A. (2018), "A simplified approach to assess seismic stability of tailings dams", *J. Rock Mech. Geotech. Eng.*, **10**(6), 1082-1090. https://doi.org/10.1016/j.jrmge.2018.06.003.
Noorzad, R. and Omidvar, M. (2010), "Seismic displacement analysis of embankment dams with reinforced cohesive shell", *Soil Dyn. Earthq. Eng.*, **30**(11), 1149-1157. https://doi.org/10.1016/j.soildyn.2010.04.023.
Pang, R., Xu, B., Kong, X., Zhou, Y. and Zou, D. (2018), "Seismic performance evaluation of high CFRD slopes subjected to near-fault ground motions based on generalized probability density evolution method", *Eng. Geol.*, **246**, 391-401. https://doi.org/10.1016/j.enggeo.2018.09.004.
Pang, R., Xu, B., Kong, X. and Zou, D. (2018), "Seismic fragility for high CFRDs based on deformation and damage index through incremental dynamic analysis", *Soil Dyn. Earthq. Eng.*, **104**, 432-436. https://doi.org/10.1016/j.soildyn.2017.11.017.
Pang, R., Xu, B., Kong, X., Zou, D. and Zhou, Y. (2018), "Seismic reliability assessment of Earth-fill dam slopes considering strain-softening of Earth-fill based on generalized probability density evolution method", *Soil Dyn. Earthq. Eng.*, **107**, 96-107. https://doi.org/10.1016/j.soildyn.2018.01.020.
Park, D.S. and Kim, N.R. (2017), "Safety evaluation of cored Earth-fill dams under high seismicity using dynamic centrifuge modelling", *Soil Dyn. Earthq. Eng.*, **97**, 345-363. https://doi.org/10.1016/j.soildyn.2017.03.020.
PEER, NGA (2010), Strong Motion Database, http://peer.berkeley.edu/smcat.
Seiphoori, A., Haeri, S.M. and Karimi, M. (2011), "Three-dimensional nonlinear seismic analysis of concrete faced Earth-fill dams subjected to scattered P, SV, and SH waves considering the dam-foundation interaction effects", *Soil Dyn. Earthq. Eng.*, **31**(5-6), 792-804. https://doi.org/10.1016/j.soildyn.2011.01.003.
Terzi, N.U. and Selcuk, M.E. (2015), "Nonlinear dynamic behavior of Pamukcay Earthfill dam", *Geomech. Eng.*, **9**(1), 83-100. https://doi.org/10.12989/gae.2015.9.1.083.
Vrymoed, J. (1981), "Dynamic FEM model of Oroville Dam" *J. Geotech. Eng. Div.*, **107**(GT8), 1057-1077.
Wang, M., Chen, J. and Xiao, W. (2018), "Experimental and numerical comparative study on gravity dam-reservoir coupling system", *KSCE J. Civ. Eng.*, **22**(10), 3980-3987. https://doi.org/10.1007/s12205-018-1434-3.
Xu, B., Wang, X., Pang, R. and Zhou, Y. (2018), "Influence of strong motion duration on the seismic performance of high CFRDs based on elastoplastic analysis", *Soil Dyn. Earthq. Eng.*, **114**, 438-447. https://doi.org/10.1016/j.soildyn.2018.08.004.
Xu, H., Zou, D., Kong, X., Hu, Z. and Su, X. (2018), "A nonlinear analysis of dynamic interactions of CFRD–compressible reservoir system based on FEM–SBFEM", *Soil Dyn. Earthq. Eng.*, **112**, 24-34. https://doi.org/10.1016/j.soildyn.2018.04.057.
Yang, X.G. and Chi, S.C. (2014), "Seismic stability of earth-rock dams using finite element limit analysis", *Soil Dyn. Earthq. Eng.*, **64**, 1-10. https://doi.org/10.1016/j.soildyn.2014.04.007.
Yazdani, Y. and Alembagheri, M. (2017), "Seismic vulnerability of gravity dams in near-fault areas", *Soil Dyn. Earthq. Eng.*, **102**, 15-24. https://doi.org/10.1016/j.soildyn.2017.08.020.
Zou, D., Xu, B., Kong, X., Liu, H. and Zhou, Y. (2013), "Numerical simulation of the seismic response of the Zipingpu concrete face Earth-fill dam during the Wenchuan earthquake based on a generalized plasticity model", *Comput. Geotech.*, **49**, 111-122. https://doi.org/10.1016/j.compgeo.2012.10.010.
Zou, D., Han, H., Liu, J., Yang, D. and Kong, X. (2017), "Seismic failure analysis for a high concrete face Earth-fill dam subjected to near-fault pulse-like ground motions", *Soil Dyn. Earthq. Eng.*, **98**, 235-243. https://doi.org/10.1016/j.soildyn.2017.03.031.
Zou, D., Han, H., Ling, H.I., Zhou, Y. and Liu, J. (2019), "An approach for the real-time slip deformation coupled with strain softening of a high Earth-fill dam subjected to pulse-like ground motions", *Soil Dyn. Earthq. Eng.*, **117**, 30-46. https://doi.org/10.1016/j.soildyn.2018.10.044.

IC